# Experiments on selective excitation of multiple-quantum transitions in NMR spectroscopy

W. S. Warren[a] and A. Pines

*Department of Chemistry, University of California and Materials and Molecular Research Division, Lawrence Berkeley Laboratory, Berkeley, California 94720*
(Received 7 October 1980; accepted 21 November 1980)

Irradiating a spin system with an appropriate sequence of phase shifted pulses excites only certain orders of multiple-quantum transitions. Using such sequences in preparation and detection produces a large signal/noise enhancement for the multiple-quantum spectra over nonselective excitation, as predicted from theory. In a previous paper the theory was presented in detail. In this paper some aspects of the theory are first outlined briefly. Experimental results are then presented demonstrating four-quantum, six-quantum, and $A$-symmetry selection in oriented benzene and eight-quantum selection in oriented 1-bromobutane. A six-quantum selective sequence applied to benzene with nonequilibrium initial reduced density matrix proportional to $I_x$ produces one- and five-quantum spectra. The $n$-quantum signal/noise enhancements are obtained and the selectivity is measured as a function of pulse sequence parameters. The behavior is that expected if one assumes that the limit to selectivity is determined by leading nonselective terms in an average Hamiltonian expansion.

## I. INTRODUCTION

The observation of normally forbidden ($\Delta M \neq 1$) NMR transitions has been shown to be of great value in extracting information from complex molecules.[1-8] Because the number of different transitions decreases as $\Delta M$ increases, multiple-quantum ($\Delta M > 1$) spectra are always simpler than the normal single-quantum spectrum. Thus, multiple-quantum spectra can be interpreted even when the normal spectrum contains many unresolvable transitions. Wide band nonselective excitation of multiple-quantum transitions, which permits the simultaneous observation of transitions with all possible values of $\Delta M$, is relatively straightforward and requires only a few pulses and delays. However, wide band excitation leaves most of the spectral intensity in the single-quantum and low multiple-quantum spectra because these spectra have the most transitions. As a result, the simple high multiple-quantum spectra are weak.

One alternative approach is to selectively excite transitions which correspond to only a few values of $\Delta M$. From the viewpoint of perturbation theory, this appears impossible without detailed knowledge of the form of the Hamiltonian, since a multiple-quantum transition occurs only with irradiation which also excites lower quantum transitions. Thus, aside from even–odd selection due to the bilinear form of certain spin operations[9] and selection in small systems where the Hamiltonian is completely known,[8] no general method of selective excitation has been proposed. In a previous letter,[10] we demonstrated that selective excitation of multiple-quantum transitions is possible, and that arbitrarily high orders can be selected without prior knowledge of the exact Hamiltonian. A theory of selective excitation, some examples of highly selective sequences, and the potential signal gain from selectivity were also presented.[11,12] In this paper, we first present some aspects of the theory, and then we present the results of experiments on two molecules (benzene and $n$-butyl bromide) which show selective excitation is generally feasible and that large signal gains can be achieved.

## II. THEORY OF SELECTIVE MULTIPLE-QUANTUM NMR

### A. General theory of selective excitation

The general theory of selective excitation of multiple-quantum coherences was described in Ref. 12. In this subsection we briefly summarize this theory. In the next subsection we discuss practical pulse sequences for selective experiments which compensate for inevitable pulse errors (inhomogeneity, finite duty cycles, and the like).

To understand how selective excitation works, we consider first the *nonselective* pulse sequences in Fig. 1, and assume that we apply them to dipole-coupled nuclear spins in a large magnetic field. The Hamiltonian is then

$$\begin{aligned}\mathcal{H}_z &= \sum_{i>j} D_{ij}(3I_{zi}I_{zj} - \mathbf{I}_i \cdot \mathbf{I}_j) \\ &\quad + \sum_{i>j} J_{ij}(\mathbf{I}_i \cdot \mathbf{I}_j) + \left(\sum_i \sigma_i I_{zi} + \Delta\omega I_z\right) \\ &\equiv \mathcal{H}_{zz} + \mathcal{H}_J + (\mathcal{H}_{cs} + \Delta\omega I_z) \ , \end{aligned} \tag{1}$$

where typically $\| \mathcal{H}_{zz} \| \gg \| \mathcal{H}_{cs} \|$, $\| \mathcal{H}_J \|$. The simplest pulse sequence for producing nonselective wide band multiple-quantum spectra is shown in Fig. 1(a).[4-6,8] The first two pulses, separated by a delay $\tau$ such that $\| \mathcal{H}_{zz}\tau \| \gtrsim 1$, constitute the preparation sequence. The initial (equilibrium) reduced density matrix is $\rho_0 = -\beta I_z$. At the end of the second pulse, the reduced density matrix is

$$\begin{aligned}\rho &= -\beta \exp(-i\pi I_y/2) \exp(-i\mathcal{H}_z\tau) \exp(i\pi I_y/2) \\ &\quad \times I_z \exp(-i\pi I_y/2) \exp(i\mathcal{H}_z\tau) \exp(i\pi I_y/2) \\ &\equiv -\beta \exp(-i\mathcal{H}_x\tau) I_z \exp(i\mathcal{H}_x\tau) \ , \end{aligned} \tag{2}$$

[a] Present address: Department of Chemistry, California Institute of Technology, Pasadena, CA 91125.

 0021-9606/81/052808-11$01.00 

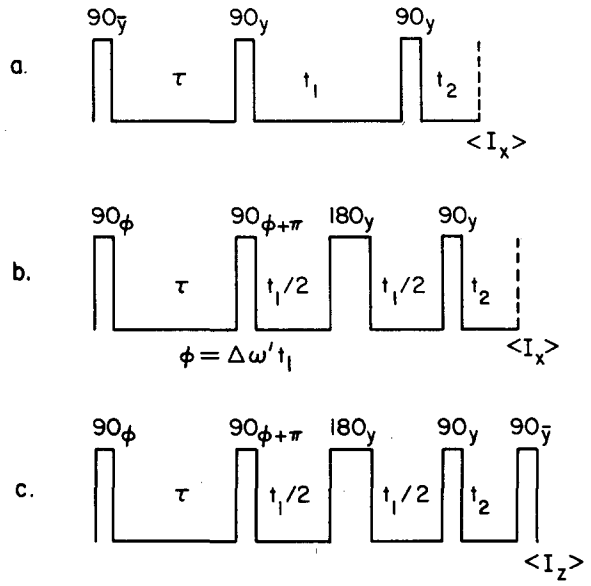


FIG. 1. Several common nonselective pulse sequences for producing multiple-quantum NMR spectra. In each sequence the density matrix after the first two pulses has multiple-quantum coherences if $\tau$ is greater than the reciprocal of a typical dipolar energy level difference.

$$\mathcal{H}_x = \sum_{i>j} D_{ij}(3I_{xi}I_{xj} - \mathbf{I}_i \cdot \mathbf{I}_j) + \sum_{i<j} J_{ij}(\mathbf{I}_i \cdot \mathbf{I}_j) + \sum \sigma_i I_{xi} + \Delta\omega I_x \,. \quad (3)$$

In general, $\mathcal{H}_x$ will contain zero-quantum, one-quantum, and two-quantum operators, and the complex exponential gives $\rho$ matrix elements corresponding to all multiple-quantum orders. After the preparation sequence, the system evolves under $\mathcal{H}_z$ for a time $t_1$, called the evolution period. Multiple-quantum coherences do not correspond to oscillating magnetization, so they cannot be directly detected, and a third pulse plus a delay $t_2$ (called the mixing sequence) are needed to partially transfer them into the observables $\langle I_x\rangle$ and $\langle I_y\rangle$. The sequence is repeated with different values of $t_1$, Fourier transformed, converted to a magnitude spectrum, and averaged with spectra corresponding to different values of $t_2$ or $\tau$ to produce the nonselective spectrum.

Inspection of $\mathcal{H}_z$ reveals that the $n$-quantum spectrum is centered at $n\Delta\omega$, so different values of $n$ will be completely separated if $\Delta\omega > \|\mathcal{H}_z\|$. However, static inhomogeneity broadens the $n$-quantum transitions $n$ times more than the single-quantum transitions. This broadening can be eliminated by echo pulses in $t_1$, but in this case the sequence in Fig. 1(a) will center all of the multiple-quantum spectra at $\omega = 0$. The sequence in Fig. 1(b) overcomes this problem by the method of time proportional phase incrementation[5,6] (TPPI). In this experiment whenever $t_1$ is incremented by $\Delta t_1$, the phases of all the pulses in the preparation period are incremented by $\Delta\phi = (\Delta\omega')\Delta t_1$. The incrementation modulates the $n$-quantum coherences by $\exp(-in\Delta\omega' t_1)$, so that the $n$-quantum spectrum is centered at $n\Delta\omega'$.

There is actually a great deal of similarity between the preparation and mixing portions of this pulse sequence, which is hidden by the experimental need to measure $\langle I_x\rangle$ or $\langle I_y\rangle$ even though the initial density matrix is proportional to $I_z$. If instead we imagine that $\langle I_z\rangle$ can be measured, as in Fig. 1(c), an additional pulse is needed at the end of $t_2$. The sequences in Figs. 1(b) and 1(c) would always give the same spectra, but in Fig. 1(c) the symmetry between preparation and mixing is apparent (if $\tau = t_2$ they are identical except for a phase shift). For this reason we will develop the theory as if $\langle I_z\rangle$ were detected. The experimental pulse sequences will always include one additional pulse immediately before detection, to sample $\langle I_x\rangle$ or $\langle I_y\rangle$.

It can be shown that the signal is maximized for $\tau = t_2$, and in this case is equal to the expectation value of the equilibrium magnetization. There are $4^N$ density matrix elements in a system with $N$ spins $\frac{1}{2}$, and the signal is divided up among all of these elements in the nonselective experiment. If the mixing and preparation sequences selectively produce only a small fraction of the allowed coherences, the signal associated with each coherence can be much larger. For example, an $N$-quantum selective sequence in an $N$-spin system can transfer magnetization from the two states with $M = \pm N/2$ directly into $N$-quantum coherence, and the potential signal gain relative to totally nonselective excitation is $N2^N$.[12]

To perform a *selective* wide band excitation we use a sequence of the type illustrated schematically in Fig. 2(a). This sequence can replace the nonselective preparation, the nonselective mixing, or both. We can start with an arbitrary cyclic sequence of pulses and delays. This sequence, which we will call a subcycle, has a total duration of $\Delta\tau_p$ and generates a propagator $U_0$. Average Hamiltonian theory[13-15] allows us to write the propagator as $U_0 = \exp(-i\mathcal{H}_0\Delta\tau_p)$, where the effective Hamiltonian $\mathcal{H}_0$ is given by a Magnus expansion of the product of the propagators for each piece of the se-

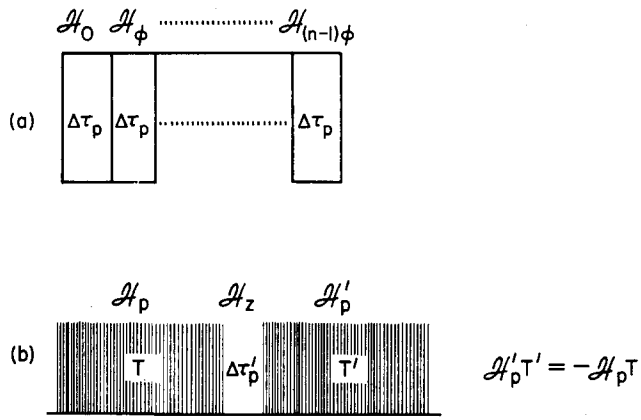


FIG. 2. General form for zero-order selective sequences. In part (a) $\mathcal{H}_0$ is an arbitrary cyclic sequence of pulses and delays. All of the pulses are phase shifted by $\phi = 2\pi/n$ to produce $\mathcal{H}_0$. To lowest order, only $nk$-quantum coherences ($k = 0, \pm 1, \pm 2, \ldots$) survive after $n$ shifts. Part (b) is a possible sequence for $\mathcal{H}_0$ which uses dipolar time reversal to give $\mathcal{H}_0$ multiple-quantum operators yet keeps $\|\mathcal{H}_0\Delta\tau_p\|$ small.

quence. The subcycle is then repeated, except all the pulses are phase shifted by an angle $-\phi$. This creates a new subcycle with a new (rotated) effective Hamiltonian:

$$\mathcal{H}_\phi = \exp(i\phi I_z)\mathcal{H}_0 \exp(-i\phi I_z) \ , \tag{4}$$

$$(\mathcal{H}_\phi)_{ij} = \exp[i(M_i - M_j)\phi](\mathcal{H}_0)_{ij} \ ,$$

which is also allowed to evolve for $\Delta\tau_p$. If $\phi = 2\pi/n$, coherences with $\Delta M = nk$ $(k = 0, \pm 1, \pm 2, \ldots)$ are unaffected, but all other coherences are multiplied by a phase factor of $\exp[i2\pi(\Delta M)/n]$. This process is repeated to make a total of $n$ phase shifts. The propagator after $n$ subcycles is

$$U = \prod_{q=0}^{n-1} \exp(-i\mathcal{H}_{\phi=2\pi q/n}\Delta\tau_p)$$

$$= 1 - i\Delta\tau_p\left(\sum_{q=0}^{n-1}\mathcal{H}_{\phi=2\pi/n}\right) + O(\|\mathcal{H}_\phi\Delta\tau_p\|^2) \ . \tag{5}$$

If $\|\mathcal{H}_\phi\Delta\tau_p\| \ll 1$, the last term can be neglected. Combining Eqs. (4) and (5) to first order in $\Delta\tau_p$ we can write

$$U_{ij} \simeq \delta_{ij} - i\Delta\tau_p\left\{\sum_{q=0}^{n-1}\exp[i2\pi q(M_i - M_j)/n]\right\}(\mathcal{H}_0)_{ij}$$

$$= \delta_{ij} - in\Delta\tau_p(\mathcal{H}_0)_{ij}\delta[(M_i - M_j) - nk] \ . \tag{6}$$

Thus $U$ will only induce transitions between states with $\Delta M = nk$, to first order in $\Delta\tau_p$. We call this a zero-order $nk$-quantum selective sequence because the zero-order average Hamiltonian is a $nk$-quantum selective operator, but all higher-order terms are nonselective. Sequences can be designed which are selective to arbitrarily high order in the average Hamiltonian expansion; these sequences are described in Refs. 11 and 12.

### B. Pulse sequences for multiple-quantum NMR

Equation (6) implies that $U$ cannot contain multiple-quantum operators unless $\mathcal{H}_0$ does, and it can be shown that no matter what the actual pulse sequence is for $\mathcal{H}_0$, it cannot contain substantial contributions from multiple-quantum operators unless $\|\mathcal{H}_z\Delta\tau_p\| \gtrsim 1$. For this reason the pulse sequence for $\mathcal{H}_0$ must be constructed such that $\|\mathcal{H}_0\| \ll \|\mathcal{H}_z\|$, or terms nonlinear in $\Delta\tau_p$ will ruin the selectivity. One particularly convenient way to do this is to use dipolar time reversal sequences as illustrated in Fig. 2(b). A pulse sequence with an effective Hamiltonian $\mathcal{H}_p$ is applied for a time $T$ such that $\|\mathcal{H}_pT\| \gtrsim 1$. After a short delay $\Delta\tau_p'$ another pulse sequence, with an effective Hamiltonian $\mathcal{H}_p'$, is applied for a time $T'$ such that $\mathcal{H}_p'T' = -\mathcal{H}_pT$. We can then write

$$U_0 = \exp(-i\mathcal{H}_0\Delta\tau_p)$$

$$= \exp(-\mathcal{H}_p'T')\exp(-i\mathcal{H}_z\Delta\tau_p')\exp(i\mathcal{H}_pT) \ , \tag{7}$$

$$\mathcal{H}_0 = (\Delta\tau_p'/\Delta\tau_p)\exp(-i\mathcal{H}_pT)\mathcal{H}_z\exp(i\mathcal{H}_pT) \ , \tag{8}$$

and if $\Delta\tau_p' \ll \Delta\tau_p$, $\|\mathcal{H}_0\| \ll \|\mathcal{H}_z\|$, yet $\mathcal{H}_0$ can have multiple-quantum coherences.

$\mathcal{H}_p$ was produced for all of the experiments in this paper by the sequence $(\tau/2 - 90_x - \tau' - 90_x - \tau - 90_{\bar{x}} - \tau' - 90_{\bar{x}} - \tau - 90_{\bar{x}} - \tau' - 90_{\bar{x}} - \tau - 90_x - \tau' - 90_x - \tau/2)$ repeated several times. The pulses have a finite width $t_p$, and we set $\tau' = 2\tau + t_p$. This sequence affects each of the three parts of $\mathcal{H}_z$ in Eq. (1) differently. The dipolar term $\mathcal{H}_{zz}$ has a zero-order average of

$$\bar{\mathcal{H}}_D^{(0)} = \tfrac{1}{3}(2\mathcal{H}_{yy} + \mathcal{H}_{zz}) = \tfrac{1}{3}(\mathcal{H}_{yy} - \mathcal{H}_{xx}) \ , \tag{9}$$

$$\mathcal{H}_{\alpha\alpha} = \sum(3I_{\alpha i}I_{\alpha j} - \mathbf{I}_i \cdot \mathbf{I}_j)D_{ij} \quad (\alpha = x, \ y, \text{ or } z) \ .$$

$\bar{\mathcal{H}}_D^{(0)}$ is purely a two-quantum operator, which means that a phase shift of 90° multiplies it by $-1$; this can also be seen by substituting $I_x \to I_y$, $I_y \to -I_x$, $I_z \to I_z$ in Eq. (9). If the pulse sequence is run with $y$ and $\bar{y}$ pulses instead of $x$ and $\bar{x}$ pulses, the zero-order average of the dipolar Hamiltonian is inverted so with this modification the sequence for $\mathcal{H}_p$ was also used for $\mathcal{H}_p'$. $\mathcal{H}_{cs} + \Delta\omega I_z$ is canceled to lowest order by this sequence, and $\mathcal{H}_J$ is unaffected. In the cases we will consider, $\|\mathcal{H}_{zz}\|$ is several orders of magnitude larger than $\|\mathcal{H}_J\|$, so $\bar{\mathcal{H}}_D^{(0)}$ dominates when $\|\mathcal{H}_zT\| \ll 1$, and very good time reversal is possible.

This sequence compensates for several common pulse errors. Static inhomogeneity would force $\Delta\omega$ to be written as $\Delta\omega(\mathbf{r})$, but the zero-order average vanishes. Similarly, rf inhomogeneity, which can be represented by a pulse flip angle of $90 - \epsilon$, does not appear in $\bar{\mathcal{H}}_D^{(0)}$ to order $\epsilon$. The largest nonvanishing error term in $\bar{\mathcal{H}}^{(0)}$ should be the cross term between static and rf inhomogeneity which is minimized by making $\Delta\omega \sim 0$.

This sequence is symmetric for the dipolar Hamiltonian, so $\bar{\mathcal{H}}_D^{(1)} = 0$. Under ideal experimental conditions, this means that the ultimate limitations to time reversal come from $\bar{\mathcal{H}}_D^{(2)}$ and $\mathcal{H}_J$, and these terms will make $\|\mathcal{H}_0\Delta\tau_p\| > \|\mathcal{H}_z\Delta\tau_p'\|$. Fortunately, one feature of the selective experiment is that perfect time reversal is unnecessary; imperfections will merely cause $\|\mathcal{H}_0\|$ to be larger than in the ideal case. If this presents a problem, $\Delta\tau_p'$ can be reduced.

## III. EXPERIMENTAL APPARATUS

All experiments were performed on a home built spectrometer with a superconducting 43 kG magnet, giving a proton resonance frequency of 182 MHz. A microprocessor-based pulse programmer produced the pulse sequences. To ensure good rf isolation, switching was done once at 30 MHz (the i.f. frequency) and once at 182 MHz. Two phases (corresponding to $x$ and $\bar{x}$) were generated by hybrids at the i.f. frequency and all phase shifts were generated by a Daico 100 D0 898 shifter.

The phases were checked with a Hewlett-Packard 8405A vector voltmeter and found to be stable, reproducible, and within ±1° of the digital setting at all times. However, the VSWR of the phase shifter depended on the phase setting. To eliminate fluctuations from this effect and from switching transients, the pulses were amplified to $\sim 3V_{pp}$ and passed through a series pair of crossed PIN diodes followed by a pair of crossed PIN diodes to ground. The first pair eliminates small components which are out of phase with the main pulse, and the second pair reduced fluctuations in the output voltage. The pulses were then filtered, amplified, and sent to the probe.

The probe had a single-tuned 8 mm i.d. × 25 mm

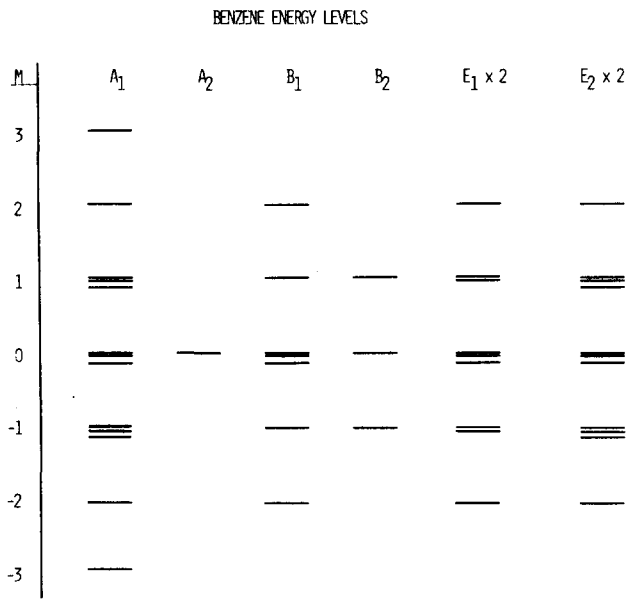


FIG. 3. Energy level diagram for benzene oriented in a liquid crystalline solvent. The assumed symmetry is $D_{6h}$. There is also a time reversal symmetry operation (flipping all spins) in the $M=0$ manifold which is not shown. This symmetry operation affects only zero-quantum transitions.

solenoidal coil. All of the samples were nematic liquid crystals, so heating effects had to be minimized. Fortunately, the selective experiment does not require signal sampling in short windows in the pulse sequence, so a high-$Q$ circuit and low power (~50 W) pulses were used. Samples were sealed in 6 mm o.d. ×15 mm Pyrex tubes, which were suspended in the center of the coil to minimize rf inhomogeneity and heating effects. A temperature-regulated air stream focused on the sample was used to further decrease heating. Even with these precautions, relatively long delays (as much as 10 sec) were sometimes required between successive shots.

## IV. EXPERIMENTAL RESULTS

### A. Oriented benzene

#### 1. *Four-quantum selection*

The high ($D_{6h}$) symmetry of benzene produces many different irreducible representations for the eigenstates (Fig. 3). This reduces the number of allowed transitions; for example, there is only one pair of five-quantum transitions, instead of the six pairs of five-quantum transitions in an unsymmetrical six-spin system. All six protons are equivalent, so we can set $\sigma_i = 0$ for all $i$ in Eqs. (1) and (3). This molecule is small enough to be studied by nonselective sequences, and all of the theoretically allowed transitions have been observed.[4,5,9]

Figure 4(a) shows the nonselective [pulse sequence of Fig. 1(b)] multiple-quantum spectra at 24.0 °C of a sample with 14 wt. % benzene dissolved in Eastman liquid crystal no. 15320. The same sample was used for all of the benzene experiments. For this experiment $\Delta\omega = 500$ Hz, and spectra corresponding to $t_2 = \tau = 4.0$, 6.0, 8.0, and 10.0 msec were averaged together. The individual lines are resolvable even in the single-quantum spectra,[16] and the three dipolar coupling constants $D_{12}$, $D_{13}$, and $D_{14}$ have been shown to be consistent with hexagonal symmetry. Figure 4(b) shows, on the same scale, the averaged results of four spectra with $4k$-quantum selection ($\phi = \pi/2$ in Fig. 2), and different values of $T$ and $\tau$. The four-quantum transitions are significantly enhanced (the integrated intensity is increased by a factor of 3.83) and their positions are unaffected. The nonselected orders are almost entirely under the noise level.

In Figs. 5 and 6 we present individual spectra (not

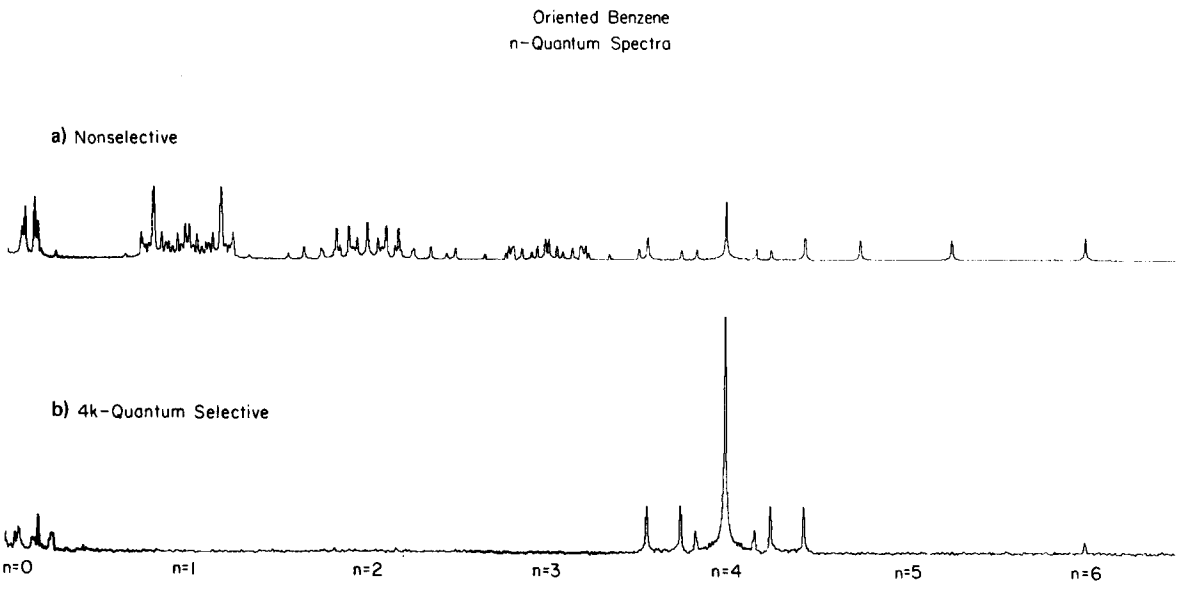


FIG. 4. Multiple-quantum ensemble averaged spectra of oriented benzene. The width of the four-quantum spectrum is 5470 ± 25 Hz. Part (a) is the nonselective spectrum [sequence of Fig. 1(b)]. Part (b) is 4k-quantum selective (sequence of Fig. 2).

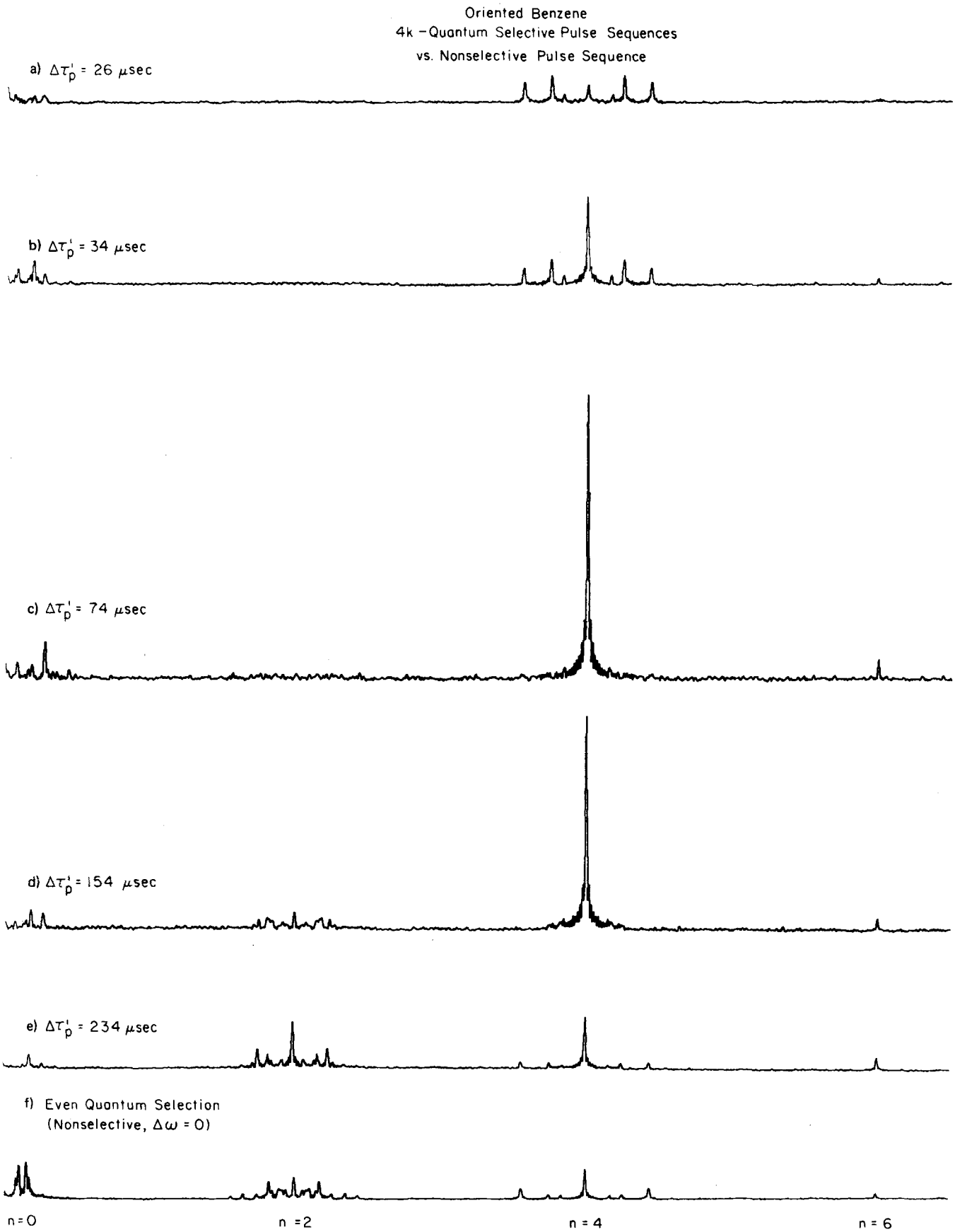


FIG. 5. The effects of varying $\Delta\tau_p'$ (see Fig. 2) in 4k-quantum selective sequences on oriented benzene. When $\Delta\tau_p'$ is long the selectivity has disappeared. The optimum value of $\Delta\tau_p'$ is expected to be longer for the central peak than for the side peaks (see the text). The largest observed gains are 5.6 for the side peaks and 19 for the central peak. Pulse sequence parameters are given in the text.

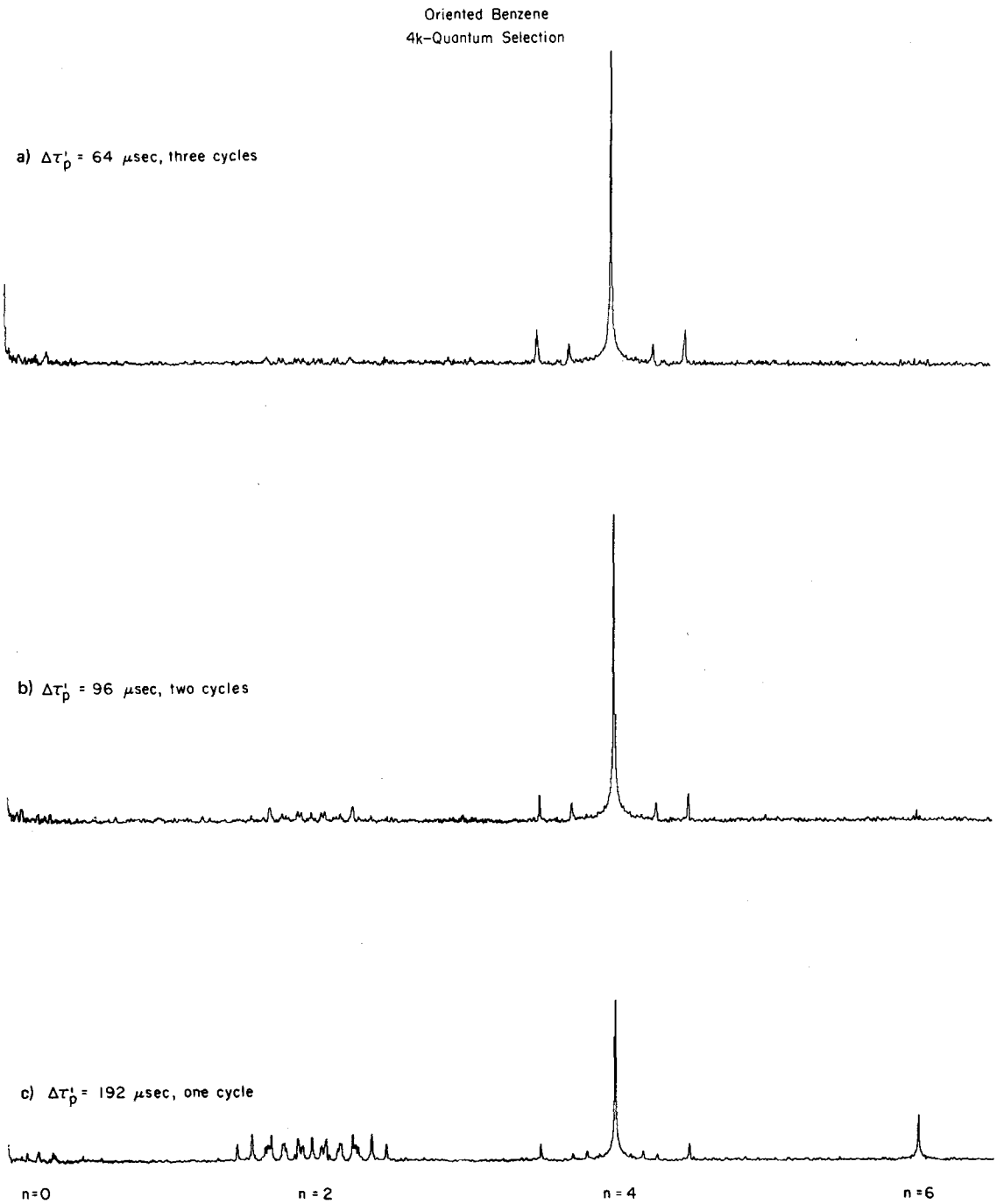


FIG. 6. The effects of increasing the cycle time and reducing the number of cycles. Average Hamiltonian theory predicts that this will not change the selective terms but will increase the nonselective terms. Pulse sequence parameters are given in the text.

averaged over any parameters in the pulse sequence) to calculate selectivity and maximum signal gains. Each of the spectra in Fig. 5 was taken with $\phi=\pi/2$, $t_p=3.8$ μsec, $\tau=5.0$ μsec, $T=1.5$ msec, and eight subcycles (the zero-order sequence was applied two consecutive times) to make a $4k$-quantum selective sequence. The sequence was used in both the preparation and mixing periods. Immediately before detecting $\langle I_x\rangle$ and $\langle I_y\rangle$, a single additional pulse was applied as explained in Sec. II A. The only parameter which was varied was $\Delta\tau_p'$.

The selective terms in the average Hamiltonian are linear in $\Delta\tau_p'$. Higher-order terms are nonselective, so the spectra with large values of $\Delta\tau_p'$ are expected to have substantial two-quantum and six-quantum intensity [$\mathcal{H}_0$ still has the form in Eq. (8), so no odd-quantum op-

erators are present in the propagator]. Figure 5(e) confirms this result. If $\Delta\tau_p'$ is very small and the time reversal is good, even the linear term is small, and very little coherence is produced. Thus, there should be an optimal value (or at least an optimal range) for $\Delta\tau_p'$ to produce four-quantum coherences. One interesting feature of Fig. 5 is that the value which optimizes the central four-quantum line is much longer than the value which optimizes the side peaks. There is no reason why the optimal values should be the same; the side peaks are all $A_1$ transitions, whereas the central peak has contributions from every irreducible representation. In addition, diagonalizing the Hamiltonian shows that $\|\mathcal{H}_z\|$ is larger for the $A_1$ states than for any other representation, so from Eq. (8) we expect that if we averaged over all possible operators $\mathcal{H}_p$, the $A_1$ transitions would peak at the smallest values of $\Delta\tau_p'$. However, this need not be true for each possible $\mathcal{H}_p$.

### 2. Signal gains from selectivity

The maximum observed signal gain for the side peaks relative to totally nonselective excitation is the gain of 5.6 in Fig. 5(b). The delay between successive shots was 4 sec, and was determined by heating effects; the nonselective experiment can be run with a slightly shorter delay (2.5 sec). The true maximum gain may be larger than this, since a small change in $\Delta\tau_p'$ from 34 $\mu$sec might produce a larger value. The maximum theoretical gain may be estimated by dividing up the total available intensity [which is the same as the equilibrium magnetization, $\beta Tr(I_z^2)$] equally among all of the pumped density matrix elements in the $A_1$ manifold. There are 13 $A_1$ states, so there are 169 matrix elements, but time-reversal symmetry in the $M=0$ manifold forces all six zero-quantum transitions in that manifold plus the three populations to vanish in the nonselective experiment.[17-19] A four-quantum selective propagator will transfer some of $\beta Tr(I_z^2)$ from ten of the populations ($M=\pm3, \pm2, \pm1$) to the 14 four-quantum coherences using only terms linear in $\Delta\tau_p'$. Only 24 matrix elements are involved, and if they are all roughly equal, the expected gain is $160/24 \sim 6.7$.

However, it is clear from the spectra in Fig. 5 that some zero-quantum coherences are also produced. This is to be expected because four-quantum operators proportional to $\Delta\tau_p'$ in the propagator imply zero-quantum and four-quantum operators proportional to $(\Delta\tau_p')^2$. There are 12 zero-quantum coherences which can be pumped, and if these are pumped as strongly as the four-quantum coherences the maximum gain falls to 4.4.

The largest enhancement observed for the four-quantum center line is the factor of 19 in Fig. 5(c). This gain cannot be readily compared to the theoretical gain because this peak corresponds to six different transitions in the different irreducible representations. In addition, the TPPI method of separating the different orders of coherence can produce artifact peaks if the phase shifts are imperfect. In this experiment, the TPPI increment was $\pi/8$ (this means that each pulse in the preparation period had its phase incremented by $\pi/8$ every time $t_1$ was incremented), so that the initial phase setting was incremented by $\pi/2$ after four points were taken in $t_1$. A phase shift of $\pi/2$ does not affect populations, zero-quantum coherences, or four-quantum coherences, so it does not affect the density matrix if the selectivity is good. Thus, phase shift inaccuracies would slightly modulate these coherences with a period of four points, producing small satellite peaks with an apparent $\Delta M$ of 0, $\pm4$, or $\pm8$. The largest peak by far in the selective experiment is at $\omega=0$ (corresponding to populations which cannot be transferred into four-quantum coherence), so the only observable effect of these imperfections is to distort the intensity of the central four-quantum peak (and produce a small central peak corresponding to $\Delta M=8$, which does not overlap with the benzene spectrum). The central four-quantum peak has no dipolar information so a distorted intensity does not affect the analysis.

Figure 5(f) shows an ensemble averaged nonselective experiment [using the pulse sequence in Fig. 1(b)] with $\Delta\omega=0$. $\mathcal{H}_x$ has only even-quantum coherences,[9] so a partially selective spectrum is produced. Comparison of Figs. 5(a)–5(e) with Fig. 5(f) shows that the selective experiment does not distort lines positions. Residual pulse errors increase the noise level of the selective experiment, but the signal-to-noise ratio of the four-quantum lines in Figs. 5(a) and 5(b) is still substantially better than could be achieved nonselectively in equal time.

### 3. Suppression of nonselective operators

The first nonselective term in the effective Hamiltonian for a zero-order selective sequence is proportional to $\Delta\tau_p'$. If $\Delta\tau_p'$ is cut in half but the number of subcycles is doubled, this term will be cut in half. The selective term will be unaffected. Thus, the selectivity of a zero-order sequence can be made arbitrarily good by making $\Delta\tau_p'$ small and repeating the sequence many times. This is illustrated in Figs. 6(a)–6(c). In this experiment $t_p=5.9$ $\mu$sec, $\tau=6.0$ $\mu$sec, $\tau'=18.2$ $\mu$sec, and $T=576$ $\mu$sec, so $\mathcal{H}_0$ is different from the sequences in Fig. 5. The selective term should be identical for each of the three spectra, and this is confirmed in Figs. 5(a) and 5(b). The four-quantum regions are virtually identical for these two spectra (this particular choice of pulse sequence parameters happens to pump two of the pairs more strongly than the third), except that the four-quantum transitions are slightly weaker in Fig. 5(b) as the reduced selectivity produces some two-quantum transitions. In Fig. 5(c) the selectivity has almost disappeared.

Figures 4, 5, and 6 show that suppression of two-quantum coherences is substantially easier than suppression of six-quantum coherences. This result is expected if the phase shifts are imperfect.[12] If the phase of the $i$th subcycle is $\phi_i+\epsilon_i$ instead of the ideal value $\phi_i$, a nonselected coherence ($\Delta M \neq nk$) is multiplied by $\{\sum \exp[i(\Delta M)(\phi_i+\epsilon_i)]\}/n$ instead of 0. If $\epsilon_i \ll 1$ this is approximately equal in magnitude to $(\Delta M)\langle\epsilon_i^2\rangle^{1/2}/n^{1/2}$, so the error term is three times worse for $\Delta M=6$ than for $\Delta M=2$. Fortunately, most of the allowed coherences correspond to small values of $\Delta M$ and are relatively insensitive to phase errors.

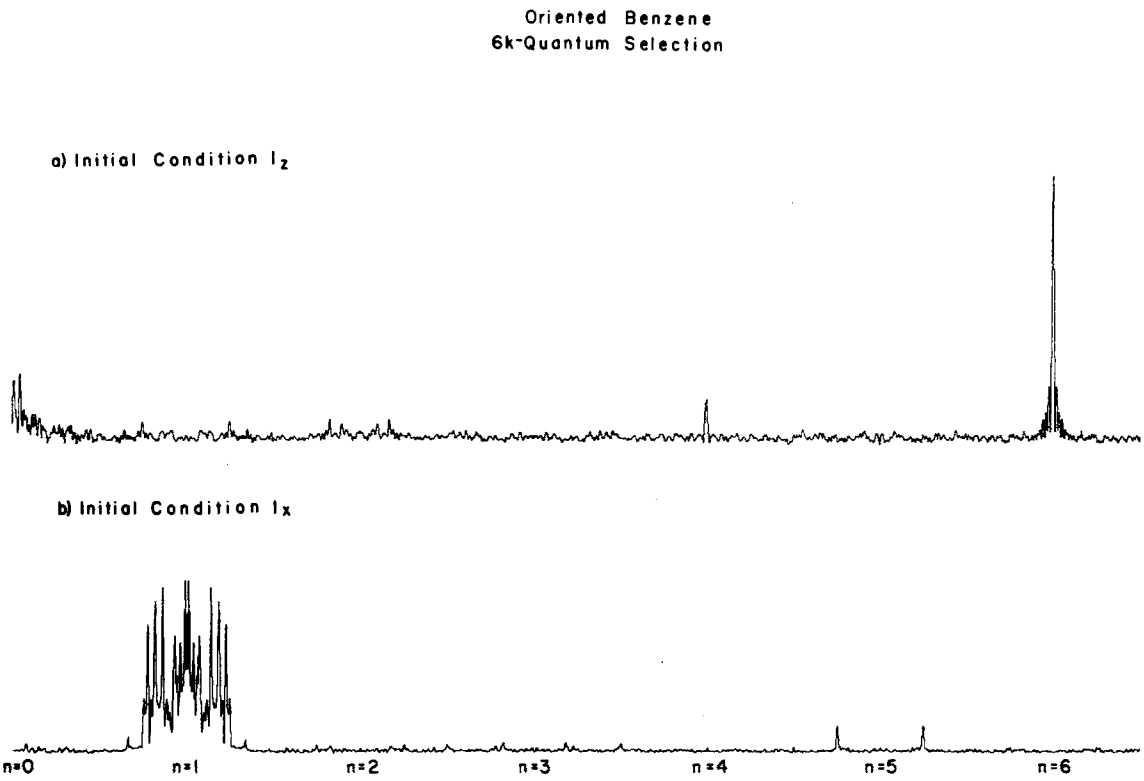


FIG. 7. Spectra with 6k-quantum selection on oriented benzene. If the initial density matrix is at equilibrium, as in part (a), only the six-quantum coherence is produced. If the initial density matrix is made proportional to $I_x$ by one pulse as in part (b), one-quantum and five-quantum coherences are produced.

### 4. *Six-quantum selection*

A $6k$-quantum selective sequence can be generated by setting $\phi = 2\pi/6$ in Fig. 2(a). If this sequence is applied to benzene at equilibrium (initial density matrix proportional to $I_z$), it connects only the states with $|M| = 3$ and creates an effective two-level system. The six-quantum spectrum which is generated has only one transition, as illustrated in Fig. 7(a). However, if the initial density matrix is made proportional to $I_x$ by adding one pulse before the selective sequence begins, a $6k$-quantum selective propagator will produce only one-quantum and five-quantum coherences. These coherences can be detected by the same $6k$-quantum selective sequence if the final pulse of the sequence is removed, and the spectrum is shown in Fig. 7(b).

The residual nonselective coherences are not completely suppressed for $6k$-quantum selection because the phase shifter described earlier can only produce shifts in exact multiples of $2\pi/256$. A zero-order sequence was approximated by $\phi$ values of 0, $43\pi/128$, $85\pi/128$, $\pi$, $171\pi/128$, $213\pi/128$ instead of 0, $\pi/3$, $2\pi/3$, $\pi$, $4\pi/3$, $5\pi/3$. This approximation leaves a small amount of non-$6k$-quantum selective operators in the zero-order term. However, the figure shows that even with this approximate sequence fairly good selectivity can be achieved.

The six-quantum signal produced from one cycle of $6k$-quantum selection as a function of $\Delta\tau_p'$ is shown in Fig. 8. If the time reversal and selectivity are perfect,

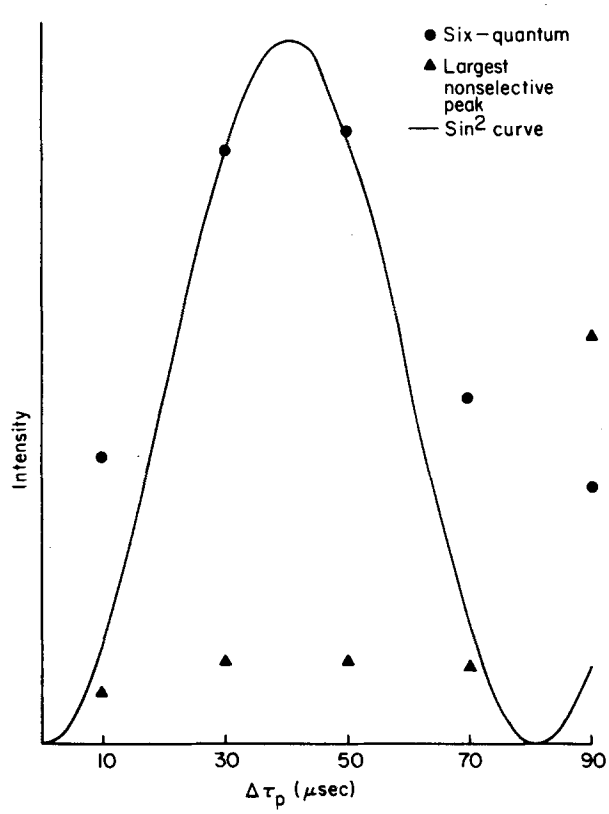


FIG. 8. Six-quantum signal as a function of $\Delta\tau_p'$. If the time reversal in $\mathcal{H}_p$ and $\mathcal{H}_p'$ is perfect, then the signal should follow a $\sin^2$ pattern. There are substantial deviations, yet good selectivity can still be achieved.

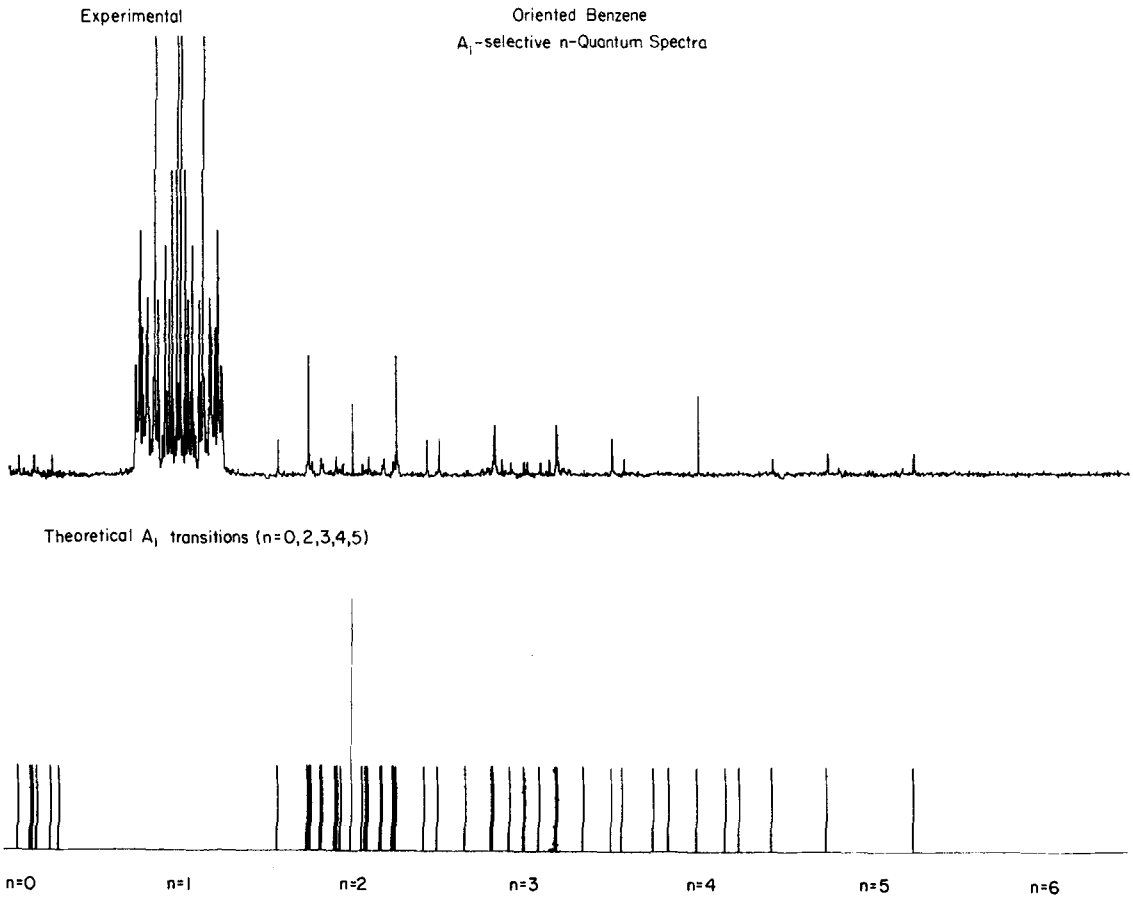


FIG. 9. $A_1$ symmetry selection on oriented benzene. 6k-quantum selection produces a density matrix which is at equilibrium in all manifolds except for $A_1$, so one additional pulse gives only single-quantum coherences in these manifolds, but multiple-quantum $A_1$ coherences.

the six-quantum signal should follow a $\sin^2$ pattern, since the six-quantum selection creates an effective two-level system.[12] Figure 8 deviates from this pattern for large values of $\Delta\tau_p'$ (where the selectivity is poor) and very short values of $\Delta\tau_p'$ (because imperfect time reversal makes $\|\mathcal{H}_0\| \neq 0$ even if $\Delta\tau_p' = 0$).

The pulse sequence parameters were $\tau = 4.5$, $t_p = 2.5$, and $T = 672$ $\mu$sec; with $t_p = 4.5$ $\mu$sec the time reversal was clearly worse, and the maximum signal was observed with $\Delta\tau_p' = 0$. Since these pulse sequence parameters are very similar to those used for four-quantum selection, it may be concluded that perfect time reversal is not needed for good selectivity and signal gains.

The single six-quantum coherence in benzene has $A_1$ symmetry, as does the single $N$-quantum transition in any $N$-spin system. Therefore, a $6k$-quantum selective sequence applied to an equilibrium density matrix perturbs only $A_1$ states; all other representations are unaffected. If a single pulse is applied immediately after the selective sequence, $A_1$ transitions corresponding to all possible values of $\Delta M$ are produced, but non-$A_1$ appear only if $\Delta M = 1$, since the density matrix in all other representations is proportional to $I_x$ or $I_y$. Such a sequence therefore selectively prepares $A_1$ multiple-quantum transitions, and at the end of the evolution period, a single pulse followed by a $6k$-quantum selective sequence selective detects $A_1$ transitions. The resulting spectrum is shown in Fig. 9. One pair of non-$A_1$ transitions is visible in the three-quantum spectrum; this pair corresponds to two nearly degenerate sets of transitions from the $E_1$ and $E_2$ manifolds, and is fairly intense in the nonselective spectrum. Except for this pair, all of the observed lines correspond to known $A_1$ transitions.

We conclude that $4k$-quantum selection, $6k$-quantum selection, and $A_1$ selection can be readily demonstrated in oriented benzene. Nonselective terms can be made very small, and the signal gain from selectivity is approximately equal to the theoretical predictions. The behavior as $\Delta\tau_p'$ or the number of cycles is varied is consistent with predictions from average Hamiltonian theory for a zero-order selective sequence.

### B. Oriented *n*-butyl bromide: Eight-quantum selection

Benzene is a small and highly symmetric molecule, so nonselective multiple-quantum spectra are perfectly adequate. However, the signal available for any individual transition in the absence of molecular symmetry is proportional to $4^{-N}$, where $N$ is the number of spins in the molecule. Thus, an unsymmetrical seven-spin molecule requires 16 times as many signal measurements as does an unsymmetrical six-spin molecule to

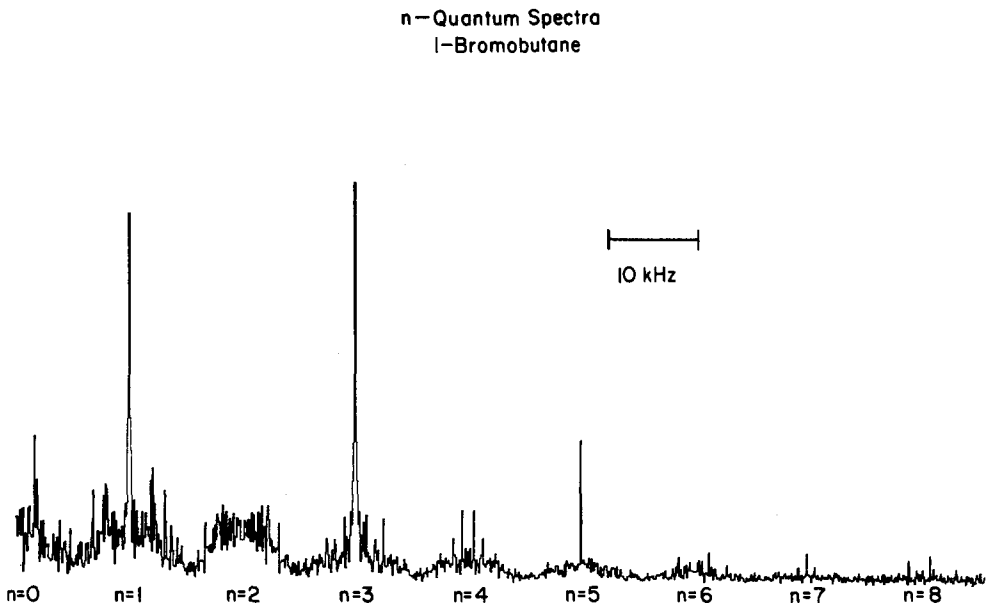


FIG. 10. Nonselective multiple-quantum spectra of 1-bromobutane. The signal intensity for the large values of $\Delta M$ is extremely small.

achieve the same signal-to-noise ratio.

This problem is illustrated in Fig. 10 with the nonselective multiple-quantum spectra of $n$-butyl bromide (1-bromobutane). The seven-quantum and eight-quantum spectra of this nine-spin system are expected to reflect internal motion of the chain.[19,20] However, these spectra are essentially unobservable, since there are many more transitions in the one-quantum and two-quantum spectra. Extensive averaging of nonselective spectra has verified that these transitions are weak.

There are 144 states with $A_1$ symmetry in $n$-butyl bromide[19,20] (2 with $|M|=9/2$, 8 with $|M|=7/2$, 26 with $|M|=5/2$, 46 with $|M|=3/2$, and 62 with $|M|=1/2$). This distribution produces four pairs of eight-quantum transitions and 19 pairs of seven-quantum transitions (simple symmetry arguments[21] show that there are three more pairs of seven-quantum transitions in the other representations). Nonselective excitation divides the total signal among $144^2=20\,736$ matrix elements. By contrast, ideal eight-quantum selective excitation would involve only 16 eight-quantum coherences, the populations of the ten states with $|M|=9/2$ or $|M|=7/2$ (no other states are connected by eight-quantum operators), and 24 zero-quantum coherences for a total of 50 matrix elements. The available signal is the fraction of $\beta T\gamma(I_z^2)$ in the ten selected populations, which is 33% of the total. The net result is a predicted maximum signal gain of 137, which reduces the signal accumulation time by a factor of 18 700. This tremendous gain would probably require high-order selective pulse sequences and suppression of zero-quantum coherences, as explained in Ref. 12. Nonetheless, even a zero-order selective sequence should give a large enhancement.

Figure 11 shows the results of averaging only four $8k$-quantum selective spectra ($\phi=\pi/4$ in Fig. 2). The TPPI increment is $\pi/16$ for these spectra so that inaccurate phase shifts are expected to produce a large central spike in the eight-quantum region. At least three of the four expected pairs can be seen. The chain has many allowed conformations, so very little information can be extracted from these few lines, and the seven-quantum spectrum will also be required. This spectrum can be obtained in two fundamentally different ways. A seven-quantum selective propagator can be designed by setting $\phi=2\pi/7$ in Fig. 2(a). Since $\mathcal{H}_0$ in Fig. 2(b) is even-quantum selective, some change has to be made in

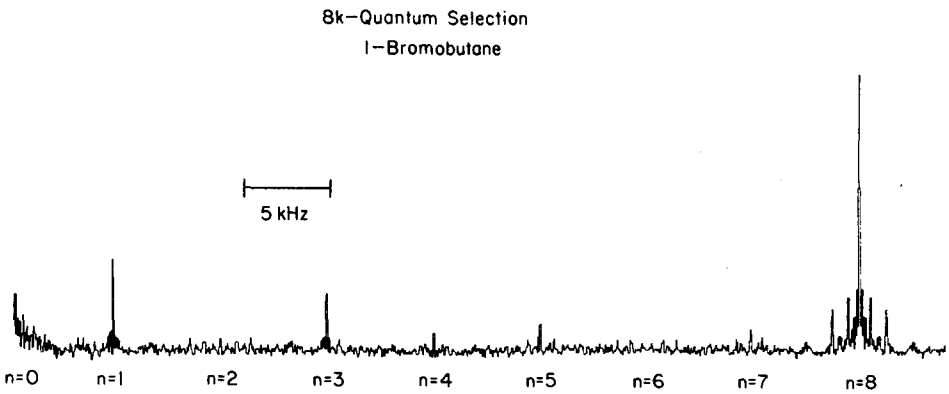


FIG. 11. The effects of 8k-quantum selection on 1-bromobutane. The signal scale is the same as in Fig. 10. At least three of the four expected pairs are visible above the noise level.

the sequence; one possibility would be to put a 45° pulse immediately before $\Delta\tau_p'$, and another 45° pulse with opposite phase immediately after $\Delta\tau_p'$. This sequence would pump all 22 pairs of seven-quantum lines. An alternative approach would be to use an eight-quantum selective pulse sequence starting with a density matrix proportional to $I_x$ instead of $I_z$. Since only the $A_1$ representation can have eight-quantum operators, only the 19 pairs of $A_1$ seven-quantum transitions, the single nine-quantum transition, and one-quantum transitions will be produced. The first approach will probably give the larger signal gain.

## V. CONCLUSIONS

Selective excitation sequences have been presented for four-, six-, and eight-quantum transitions. These sequences produce large signal enhancements and make multiple-quantum NMR a practical technique for a wide range of hitherto inaccessible molecules. The effects of changing pulse sequence parameters agree with predictions based on average Hamiltonian theory, which suggests that more sophisticated pulse sequences selective to higher order will be able to provide further signal enhancement.

## ACKNOWLEDGMENTS

We wish to thank Gary Drobny for his help with the $n$-butyl bromide experiment and for construction of the phase box controller, and Kathleen Warren for typing the manuscript. This work was supported by the Division of Materials Sciences, Offices of Basic Energy Sciences, U. S. Department of Energy under contract No. W-7405-Eng-48. W.S.W. holds a National Science Foundation Graduate Fellowship.

[1]H. Hatanaka, T. Terao, and T. Hashi, J. Phys. Soc. Jpn. **39**, 835 (1975).
[2]H. Hatanaka and T. Hashi, J. Phys. Soc. Jpn. **39**, 1139 (1975).
[3]S. Vega, T. W. Shattuck, and A. Pines, Phys. Rev. Lett. **37**, 43 (1976).
[4]A. Pines, D. Wemmer, J. Tang, and S. Sinton, Bull. Am. Phys. Soc. **23**, 21 (1978).
[5]G. Drobny, A. Pines, S. Sinton, D. P. Weitekamp, and D. Wemmer, Faraday Symp. Chem. Soc. **13**, 49 (1979).
[6]G. Bodenhausen, R. L. Vold, and R. R. Vold, J. Magn. Reson. **37**, 93 (1980).
[7]M. E. Stoll, A. J. Vega, and R. W. Vaughan, J. Chem. Phys. **67**, 2029 (1977).
[8]W. P. Aue, E. Bartholdi, and R. R. Ernst, J. Chem. Phys. **64**, 2229 (1976); A. Wokaun and R. R. Ernst, Chem. Phys. Lett. **52**, 407 (1977); A. Wokaun and R. R. Ernst, Mol. Phys. **36**, 317 (1978).
[9]D. Wemmer, Ph.D. thesis, University of California, Berkeley, 1979 (published as Lawrence Berkeley Laboratory report LBL-8042); G. Drobny, D. Wemmer, J. Tang, and A. Pines (to be published).
[10]W. S. Warren, S. Sinton, D. P. Weitekamp, and A. Pines, Phys. Rev. Lett. **43**, 1791 (1979).
[11]W. S. Warren, D. P. Weitekamp, and A. Pines, J. Magn. Reson. **40**, 581 (1980).
[12]W. S. Warren, D. P. Weitekamp, and A. Pines, J. Chem. Phys. **73**, 2084 (1980).
[13]U. Haeberlen and J. S. Waugh, Phys. Rev. **175**, 453 (1968).
[14]U. Haeberlen, *High Resolution NMR in Solids, Selective Averaging* (Academic, New York, 1976).
[15]M. Mehring, *High Resolution NMR Spectroscopy in Solids* (Springer, Berlin, 1976).
[16]A. Saupe, Z. Naturforsch. Teil A **20**, 572 (1965).
[17]All of the $A_1$ $M=0$ states are *gerade*. The density matrix in Eq. (2) only connects *gerade* to *ungerade* in the $M=0$ manifold, so no zero-quantum coherences are produced. If $M\neq 0$, there is not time reversal symmetry.
[18]J. Murdoch, W. S. Warren, and A. Pines (to be published).
[19]D. Weitekamp (private communication).
[20]G. Drobny (private communication); G. Drobny, D. P. Weitekamp, W. S. Warren, and A. Pines, Chem. Phys. Lett. (submitted).
[21]W. S. Warren and A. Pines, J. Am. Chem. Soc. (in press).